Journal of Materials Chemistry B

Accepted Manuscript

This article can be cited before page numbers have been issued, to do this please use: J. L. Paris, G. Villaverde, V. CABAÑAS, M. Manzano and M. Vallet-Regi, *J. Mater. Chem. B*, 2018, DOI: 10.1039/C8TB00444G.

ROYAL SOCIETY OF CHEMISTRY

rsc.li/materials-b

View Article Online
DOI: 10.1039/C8TB00444G

Journal Name

ARTICLE

From Proof-of-Concept Material to PEGylated and Modularly Targeted Ultrasound-Responsive Mesoporous Silica Nanoparticles.

Received 00th January 20xx,
Accepted 00th January 20xx

DOI: 10.1039/x0xx00000x

www.rsc.org/

Juan L. Paris[a,b], Gonzalo Villaverde[a,b], M. Victoria Cabañas[a], Miguel Manzano[a,b] and María Vallet-Regí[a,b,*]

In this work we present the synthesis, characterization and *in vitro* biological evaluation of PEGylated and actively-targeted ultrasound-responsive hybrid mesoporous silica nanoparticles. This work covers the development of the chemical strategies necessary to afford a modular nanocarrier starting from a proof-of-concept material presented in previous work. This functional ultrasound-responsive material can be adapted to different specific pathological conditions by carefully choosing the appropriate targeting moieties. The new ultrasound responsive material is able to target HeLa cells when conjugated with biotin or an RGD peptide. Ultrasound-responsive cytotoxicity towards cancer cells of doxorubicin-loaded nanoparticles is demonstrated in an *in vitro* cytotoxicity assay.

Introduction

Nanomedicine, the use of nanotechnology to diagnose or treat different pathologies, holds great promise to improve patient care.[1] Almost 75% of nanomedicines in clinical use consist of nanoparticles for drug delivery,[2] in which the main rationale is their capacity to improve the pharmacokinetics of the drug. Nanocarriers can enhance the stability and circulation time of the drug, increasing the amount that reaches the target organ and, therefore, decreasing the toxicity of chemotherapeutic drugs[1]. In the context of cancer, nanoparticles are able to reach tumor tissues due to the enhanced permeation and retention (EPR) effect.[3] The EPR effect is based on an increased extravasation of nanoparticles and macromolecules into the tumor due to leaky vasculature in the area, coupled with a decreased withdrawal capacity caused by the collapse of lymphatic vessels in solid tumors. Decorating the nanoparticle surface with polyethylene glycol (PEG) chains, in a process so-called PEGylation, inhibits protein adsorption on the nanoparticle surface. This hinders its recognition by macrophages and increases their circulation time in the bloodstream. This allows more nanoparticles to reach the tumor site. Additionally, active targeting strategies have also been developed by decorating the surface of nanocarriers with molecules that will induce their selective internalization in cancer cells.[4] This active targeting has been shown to increase the therapeutic efficacy of nanomedicines.[4]

In recent years, stimuli-responsive nanomaterials have attracted great attention in the context of cancer treatment.[5] The possibility of inducing drug release only in the diseased site could potentially improve the efficacy of nanotherapeutics while decreasing the side-effects of systemic administration of anticancer drugs. Both internal (like pH or redox)[6,7] and external (like light, magnetic field and ultrasound)[8–18] stimuli have been widely studied. However, ultrasound (US) appears especially interesting due to its non-invasiveness and high penetration capacity in living tissues. US offers the possibility to focus high frequency ultrasound deep into the body and the tumor mass, which would avoid unnecessary exposure to surrounding healthy tissues.[10]

Mesoporous Silica Nanoparticles (MSNs) have also attracted much attention as drug carriers due to their high physicochemical stability and textural properties that would allow a high drug loading capacity.[19–23] In our group, we have recently reported an US-responsive MSN-based drug nanocarrier as an efficient proof of concept system for on-demand drug delivery.[24] However, the material presented in our previous work lacked some of the necessary characteristics needed for its use in a therapeutic application. For example, the surface of the material at physiological temperature is highly hydrophobic and the particles tend to aggregate. The lack of a PEG layer and active targeting moieties would also prevent them from reaching the desired target cancer cells.[25,26]The objective of this work is to adapt our previous proof-of-concept material to a more viable design, according to the current knowledge in the field. Consequently, a series of

[a] Dpto. Química en Ciencias Farmacéuticas, Facultad de Farmacia, Universidad Complutense de Madrid; Instituto de Investigación Sanitaria Hospital 12 de Octubre (imas12), 28040-Madrid,Spain.
[b] Centro de Investigación Biomédica en Red de Bioingeniería, Biomateriales y Nanomedicina(CIBER-BBN), Spain
*Corresponding author: vallet@ucm.es
Electronic Supplementary Information (ESI) available. See DOI: 10.1039/x0xx00000x

View Article Online
DOI: 10.1039/C8TB00444G

chemical strategies were here developed to synthesize a PEGylated and modularly targeted US-responsive nanomaterial.

Experimental

Materials.

The following compounds were purchased from Sigma-Aldrich, and were used without further purification: ammonium nitrate, tetraethyl orthosilicate (TEOS), pyridine, methacrylic acid (MAA), (3-aminopropyl)triethoxysilane (APTES), cetyltrimethylammonium bromide (CTAB), fluorescein isothiocyanate (FITC), p-toluenesulfonic acid, dichloromethane (DCM), dihydropyran (DHP), dibenzocyclooctyne-amine (DBCO-amine), dimethylformamide (DMF), 2-(2-methoxyethoxy) ethyl methacrylate (MEO2MA), 4,4'-azobis(4-cyanovaleric acid) (ABCVA), diethyl ether, hexylamine, N-hydroxysuccinimide (NHS), N,N-diisopropylethylamine (DIPEA), 4-cyano-4-[(dodecylsulfanylthiocarbonyl)sulfanyl]pentanoic acid (CDTPA), triethylamine (TEA), N,N'-dicyclohexylcarbodiimide (DCC), phosphate-buffered saline (PBS), methoxypolyethylene glycol maleimide (MAL-PEG-OMe), toluene, poly(ethylene glycol) [N-(2-maleimidoethyl)carbamoyl]ethyl ether 2-(biotinylamino)ethane average M_n 3800 Da (MAL-PEG-BIOTIN), poly(ethylene glycol) (N-hydroxysuccinimide 5-pentanoate) ether N'-(3-maleimidopropionyl)aminoethane average M_n 4000 Da (MAL-PEG-NHS), 4-hydroxyazobenzene-2-carboxylic acid (HABA)/avidin kit, doxorubicin and fluorescein sodium salt. TetramethylrhodamineAzide (TAMRA-N3) was purchased from Thermo Fisher Scientific, and used without further purification. Dulbecco's Modified Eagle's Medium (DMEM), penicillin–streptomycin, and trypsin–EDTA were purchased from Invitrogen (Fisher Scientific, Spain). Fetal bovine serum (FBS) was purchased from Biowest (Labclinics, Spain).

Characterization techniques.

Characterization of the materials used in this study was performed by the following techniques: thermogravimetry and differential thermal analysis (TGA/DTA) in a PerkinElmer Pyris Diamond TG/DTA analyzer, with 10 ºC/min heating ramps, from 25 ºC to 600 ºC. Fourier transform infrared (FTIR) spectra were obtained in a Nicolet Nexus spectrometer (Thermo Fisher Scientific) equipped with a Smart Golden Gate attenuated total reflectance (ATR) accessory. Transmission electron microscopy (TEM) was carried out in a JEOL JEM 2100 instrument operated at 200 kV, equipped with a CCD camera (KeenView Camera). Phosphotungstic acid (PTA) was used to stain organic matter in the hybrid materials. N_2 adsorption was carried out on a Micromeritics ASAP 2010 instrument; surface area was obtained by applying the Brunauer–Emmett–Teller (BET) method to the isotherm and the pore size distribution was determined by the Barrett–Joyner–Halenda (BJH) method from the desorption branch of the isotherm. Mesopore diameter was obtained from the maximum of the pore size distribution curve. Z potential and hydrodynamic size of nanoparticles by Dynamic Light Scattering (DLS) were measured by means of a Zetasizer Nano ZS (Malvern Instruments) equipped with a 633 nm "red" laser. ^{1}H Nuclear Magnetic Resonance (NMR) experiments were carried out in a Bruker AV 250 MHz apparatus. Mass spectra were acquired with a Voyager DE-STR Biospectrometry Matrix-Assisted Laser Desorption/Ionization-Time Of Flight (MALDI-TOF) mass spectrometer. To determine the molecular weight distribution of the copolymers, Gel Permeation Chromatography (GPC) was performed in a Waters Alliance automatic analysis system with a Model #2695 separations module coupled to a Model #2414 Refractive Index Detector. GPC measurements were carried out using polyethylene (Glycol/ Oxide) standards and DMF with LiCl 10 mM as the eluent.

The Lower Critical Solution Temperature (LCST) of the polymers was determined by DLS by means of the drastic change in the scattering intensity obtained by the precipitation of the polymer at the LCST (determined as the temperature at which the scattering intensity is 50 % of the maximum). To determine the transition temperature, the temperature dependence of the scattering intensity of a polymer solution was measured. The temperature was increased by discrete temperature increments in the range 10-45 ºC.

Fluorescence spectrometry was used to determine cargo release by means of a Biotek Synergy 4 device. Fluorescence microscopy was performed in an Evos FL Cell Imaging System equipped with tree Led Lights Cubes (λ_{Ex} (nm); λ_{Em} (nm)): DAPI (357/44; 447/60), GFP (470/22; 525/50), RFP (531/40; 593/40) from AMG (Advance Microscopy Group). Quantitative analysis of cellular uptake was performed by flow cytometry in a BD FACSCalibur™ cytometer, and results were processed using Flowing Software.

Preparation of PEGylated Ultrasound-Responsive system.

Synthesis of Mesoporous Silica Nanoparticles.

MSNs were synthesized by a condensation reaction of TEOS in the presence of CTAB template under dilute, basic conditions, as described elsewhere.[24] FITC-labeled MSNs were synthesized by reacting 1 mg of FITC with 2.2 µL APTES in 100 µL ethanol for 2 h. Then, the reaction mixture was added with TEOS to obtain the FITC-labeled MSNs, following the same protocol as before.

Synthesis of Ultrasound-Responsive Copolymer.

The monomer tetrahydropyranyl methacrylate (THPMA) was synthesized and purified as previously described.[24,27]

The random copolymer poly(2-(2-methoxyethoxy) ethyl methacrylate-co-2-tetrahydropyranyl methacrylate), with two functional ends and a monomer ratio 90:10 (MEO_2MA:THPMA), was obtained by Reversible Addition-Fragmentation Chain Transfer (RAFT) polymerization, adding CDTPA, ABCVA, MEO_2MA and THPMA in a Schlenk flask. The flask was purged with N_2 and 8 mL dry DMF were added, with a catalytic amount of DIPEA to protect THPMA from degradation during the synthesis. Then, the flask was deoxygenated by three freeze-pump-thaw cycles. The reaction mixture was placed at 80 ºC under N_2 overnight with magnetic

View Article Online
DOI: 10.1039/C8TB00444G

stirring. The obtained polymer was then precipitated and washed with diethyl ether. During synthesis optimization, different monomers/CDTPA ratios (Table S1) were used to obtain US-responsive polymers (PUS, Figure 1) with different molecular weights. Depending on the length of the polymers, each specific sample was named as follows: ca. 25000 Da (small, PUSS), ca. 50000 Da (medium, PUSM) and ca. 70000 Da (large, PUSL). The synthesized polymers presented yellow color due to the presence of the trithiocarbonate group from the RAFT agent, which confirmed the integrity of CDTPA through the polymerization reaction.[28,29]

Preparation of PEGylated Ultrasound-Responsive Copolymer.

PEGylation of the obtained RAFT random copolymers was carried out by reacting MAL-PEG-OMe with the copolymer after the aminolysis of the trithiocarbonate group from CDTPA, which gives rise to a thiol moiety that reacted with the maleimide through a thiol-ene click reaction. This was performed as a one-pot reaction, by adding the MAL-PEG-OMe to the solution where the aminolysis was going to take place. Three PUS-PEG samples were obtained, PUS_S-PEG, PUS_M-PEG and PUS_L-PEG, depending on the PUS used. The conditions to obtain PUS_L-PEG were: 500 mg of PUS_L and 100 mg of MAL-PEG-OMe were dissolved in 14 mL of dry DMF under inert atmosphere. The solution was deoxygenated by bubbling N_2. Then, 500 µL of dry DMF containing 5 µL of hexylamine and 5 µL of TEA were added (to obtain PUS_M-PEG and PUS_S-PEG, the amount of MAL-PEG-OMe, hexylamine and TEA were adjusted to keep the same molar ratios as described above). The reaction took place overnight at room temperature, under N_2 and with magnetic stirring. Then, the polymers were precipitated in diethyl ether. After evaporating the ether, the solid was dissolved in ice-cold water. After heating the solution to 50 ºC, the precipitate formed was centrifuged and washed with preheated water. The purified polymer was then freeze-dried to obtain PUS-PEG.

Grafting PEGylated Ultrasound-Responsive Copolymer to MSNs.

Polymer grafting on the surface of MSNs to obtain HYBRID-PEG was performed as described previously.[24] Depending on the molecular weight of the polymeric gate being grafted, three different materials were obtained: $HYBRID_S$-PEG, $HYBRID_M$-PEG and $HYBRID_L$-PEG. To prepare $HYBRID_L$-PEG, 200 mg of PUS_L-PEG were conjugated with APTES (5 µL) using DCC (4 mg) and NHS (2 mg) under N_2 in 3 mL dry DMF at room temperature, overnight, under magnetic stirring. Then, this sililated copolymer was reacted with previously dispersed MSNs (35 mg) in toluene at 80 ºC, overnight. The addition of the polymer to the MSNs suspension in toluene was performed in three steps, leaving 4 h gaps between additions to prevent polymer-to-polymer condensation. The hybrid nanoparticles so obtained, $HYBRID_L$-PEG, were then collected by centrifugation and washed with toluene, DMF (3 times), cold water (3 times) and ethanol. Then, the nanoparticles were dried under vacuum. To obtain $HYBRID_M$-PEG and $HYBRID_S$-PEG, the amount of APTES, DCC and NHS were adjusted to keep the same molar ratios as used above.

Preparation of Actively-targeted PEGylated Ultrasound-Responsive system.

Synthesis of Biotin-targeted nanoparticles.

The polymer PUS_L-PEG-BIOTIN was synthesized in a similar way to the one described for PUS-PEG, grafting MAL-PEG-BIOTIN to the US-responsive copolymer PUS_L obtained by RAFT. Then, this polymer containing biotin was reacted with MSNs to obtain $HYBRID_L$-PEG-BIOTIN, in a similar way as described above. In this case, half of the polymer chains had the moiety of interest, while the other half were PUS-PEG chains without further modification.

Synthesis of RGD-targeted nanoparticles.

The synthesis of the material $HYBRID_L$-PEG-RGD was carried out in two steps: First, we prepared the hybrid containing DBCO moieties (HYBRIDL-PEG-DBCO), which was then reacted with an azide-functionalized peptide containing the RGD sequence: N3-Lys-Cys-Arg-Gly-Asp-Arg (RGD-N3).

HYBRIDL-PEG-DBCO: The polymer dibenzocyclooctyne-polyethilenglicol-maleimide, MAL-PEG-DBCO, was synthesized as follows (Scheme 1): 14 mg of DBCO-amine derivate were dissolved in the minimum amount possible of methylene chloride anhydrous. Under inert atmosphere, 10 µL of DIPEA were added and the mixture was stirred 30 minutes at room temperature (solution A). On the other hand, 40 mg of MAL-PEG-NHS were also dissolved in the minimum amount of dichloromethane under nitrogen atmosphere (solution B). Solution A was added dropwise over solution B and the resulted mixture was stirred overnight at 40 ºC. The methylene chloride was removed under vacuum and the resulting crude was purified by silica flash column chromatography using DCM:MeOH (30:1) as eluent. The final product was characterized by ^{1}H NMR, and the spectrum can be found in Figure S1.

Then, PUSL-PEG-DBCO was synthesized in a similar way as described for PUSL-PEG-BIOTIN, by grafting the synthesized MAL-PEG-DBCO to the US-responsive copolymer PUSL obtained by RAFT. This PUSL-PEG-DBCO was reacted with MSNs to obtain the HYBRIDL-PEG-DBCO similarly as described for the preparation of the hybrid containing biotin.

$HYBRID_L$-PEG-RGD: Initially, the peptide RGD-N_3 was synthetized following the standard solid-phase techniques using Fmoc-coupling chemistry (Scheme S2). Amino acids were added sequentially to build the peptide sequence on a solid resin. After the coupling of each amino acid, the solid resin was washed and deprotection of the last amino acid incorporated was performed to allow the coupling of the next one. The final functionalized Wang resin was treated with TFA/TIPS/H_2O cleavage cocktail in order to afford a peptide crude that was purified by G-25 Sephadex column size exclusion chromatography. ^{1}H NMR spectrum can be found in Figure S2.

To obtain RGD-modified particles, $HYBRID_L$-PEG-RGD, 4 mg of $HYBRID_L$-PEG-DBCO nanoparticles were reacted with RGD-N_3 (2 mg) in water at 4 ºC under magnetic stirring overnight. Then, the nanoparticles were collected by centrifugation and

View Article Online
DOI: 10.1039/C8TB00444G

washed once with cold water and twice with preheated PBS (37 ºC).

Cargo loading and release.

Fluorescein loading was performed by dispersing the HYBRID-PEG material (10 mg) in a solution of fluorescein (100 mg) in PBS (5 mL) and stirring overnight at 4 ºC, since the polymeric gate will be open at that temperature. The medium was then heated to 37 ºC and the particles were collected by centrifugation. The loaded nanoparticles were extensively washed with PBS at 37 ºC.

Doxorubicin loading was performed in a similar way using RGD-targeted nanoparticles: 4 mg of $HYBRID_L$-PEG-RGD were loaded with doxorubicin in 2.5 mL of PBS containing 1 mg/mL of the drug at 4 ºC overnight.

Release experiments were performed as follows: Fluorescein-loaded materials dispersed in PBS were exposed to a commercial laboratory ultrasound device before starting the experiment (1.3 MHz, 100 W, 10 min, continuous wave (CW), conditions used in our previous work).[24] The experiment was carried out placing aliquots of suspensions of the loaded material in 12 well plate Transwell inserts (0.5 mL per insert), and adding 1.5 mL PBS to the outer volume of the well. At each time point, the external volume was collected and analyzed, and the well was filled with 1.5 mL of fresh PBS (to ensure sink conditions). The samples were measured by fluorimetry to determine the amount of fluorescein released (λ_{Ex}: 490 nm; λ_{Em}: 514 nm). Same procedure was carried out with samples without US exposure.

Cell culture experiments.

Cell culture experiments with HeLa cells were carried out to evaluate nanoparticle uptake by the cells, as well as cell viability when incubated with drug-loaded nanoparticles. HeLa cells were seeded in 24 well plates at a density of 20,000 cells per cm^2 24 h before the experiments were performed.

For the nanoparticle uptake experiments, cells were incubated with 200 µg/mL suspension of the nanoparticles (with or without the targeting moiety) in complete culture medium (DMEM with 10% FBS). The particles were incubated with the cells overnight, and then they were removed and the cells were washed with PBS to remove non-internalized nanoparticles. Cellular uptake was evaluated by fluorescence microscopy and flow cytometry. For the fluorescence microscopy experiments, cells were fixed with methanol containing 1 µg/mL DAPI to stain the cell nuclei, followed by three washing steps with PBS. Flow cytometry experiments were performed in 0.5 % trypan blue (in PBS) to remove any extracellular fluorescence due to non-internalized nanoparticles.

For the cytotoxicity experiment, RGD-targeted nanoparticles ($HYBRID_L$-PEG-RGD), loaded with doxorubicin were incubated with the cells overnight (100 µg/mL suspension). Then, the cells were rinsed with PBS, and half of the wells were exposed to ultrasound (using a physiotherapy device, New Pocket Sonovit, New Age Italia Srl, Italy) from the top of the well totally filled with culture medium (1 MHz, 3 W/cm^2, 5 min, CW). The cells were then further incubated with 1 mL of complete culture medium per well. At different time points, cell viability was evaluated by Alamar Blue assay (Promega, Spain) following the manufacturer's instructions.

Results and Discussion

PEGylated Ultrasound-Responsive system

Recently, we have developed an ultrasound-responsive hybrid Mesoporous Silica Nanocarrier (HYBRID) capable of inducing cargo release when exposed to high frequency ultrasound.[24] That material was obtained by grafting a thermo-and ultrasound-responsive random copolymer, p(MEO_2MA-co-THPMA), to the surface of MCM 41-type MSNs. Before ultrasound exposure, the copolymer shows an LCST lower than 37 ºC, so the polymer will be collapsed on the nanoparticle surface, capping the pore entrances and avoiding premature release of the cargo. Upon US exposure, the US-sensitive monomer THPMA will be cleaved, giving rise to hydrophilic methacrylic acid. This will induce an increase in the LCST of the polymer, which will irreversibly change to a coil-like conformation, opening the pore outlets and inducing cargo release at physiological temperature.[24,30]

However, that proof-of-concept material presents several problems when considering an *in vivo* scenario. First, the polymeric gate closes the pore entrances of the material when collapsing on its surface due to the thermoresponsive behavior of the polymer.[24] This implies that, when the material is closed, the surface is highly hydrophobic and the particles would therefore be likely to aggregate. Second, this material also lacks of any type of active targeting moieties, which are thought to be of great importance for the efficacy of nanotherapeutics.[4] Both problems could be potentially addressed by the attachment of PEG chains with a targeting agent to the exposed end of the polymer. The aim of this work is to adapt the proof-of-concept material previously reported to a more useful platform, PEGylated and actively targeted. However, the chemical strategies employed in our previous work would not enable to carry out this modification in an easy fashion, so novel methods need to be explored.

A bifunctional US-responsive copolymer must be obtained to be able to attach a PEG molecule to it. That way, one functional end will be used to graft a PEG chain while the other one will be attached to the nanoparticle surface. The polymer described in our previous work,[24] which was obtained by Free Radical Polymerization (FRP), only presented one functional end, with a carboxylic acid provided by the initiator ABCVA. An US responsive copolymer with two different functional ends (PUS) has been here obtained changing the synthetic procedure from FRP to Reversible Addition-Fragmentation Chain Transfer (RAFT) polymerization by using a trithiocarbonate RAFT agent (CDTPA) that also presents a carboxylic acid (Figure 1). The monomer ratio was kept at 90:10 (MEO_2MA:THPMA) according to our previous results.[24] ^{1}H NMR spectra (Figure S3) confirmed the correct synthesis of the desired copolymers.

View Article Online
DOI: 10.1039/C8TB00444G

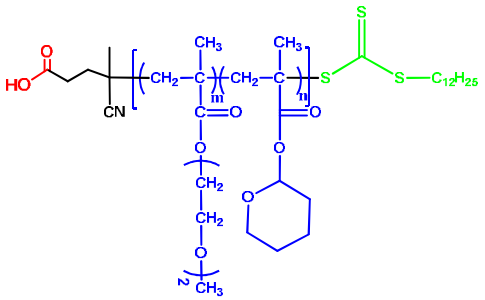

Figure 1. Structure of the obtained US-responsive polymer, PUS, obtained by RAFT polymerization.

US-Responsive copolymers, PUS, with different molecular weights (M_n) were obtained (PUS_S, PUS_M and PUS_L) by modifying the monomers/RAFT agent ratio,[31] as shown in Table 1. This allowed us to evaluate the effect of the molecular weight of the polymeric gate on the behavior of the final material.

Table 1. GPC data of the different PUS obtained in this work before and after coupling with MAL-PEG-OMe (PUS-PEG)

PUS sample	M_n (Da)	PDI	PUS-PEG sample	M_n (Da)	PDI	PEG M_n (Da)
PUS_S	25624	1.19	PUS_S-PEG	26599	1.22	2000
PUS_M	46776	1.56	PUS_M-PEG	51880	1.68	5000
PUS_L	67030	1.63	PUS_L-PEG	73061	1.78	5000

The aminolysis of the trithiocarbonate was carried out in the presence of a maleimide-modified PEG to graft it to the above RAFT copolymers. A one-pot thiol-ene click reaction took place, coupling the PEG chain to our US-responsive copolymers,[29] obtaining PUS-PEG polymers (Scheme 1) with different molecular weights (Table 1).

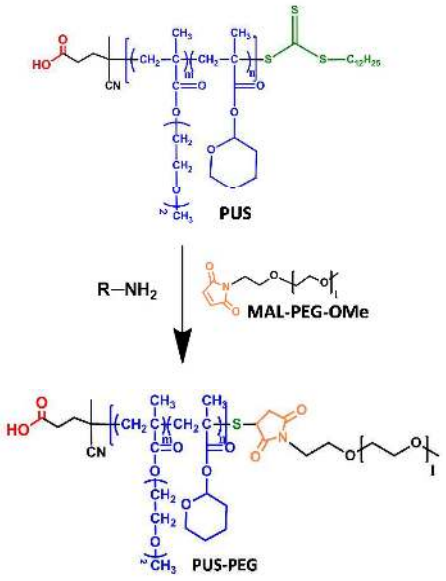

Scheme 1. Representation of the synthetic procedure employed to obtain PUS-PEG.

After purification, the ^{1}H NMR spectra of the obtained copolymers (Figure S3) confirms the PEG grafting (signal between 3.6 and 3.7 ppm). Table 1 shows an increase in the molecular weight of the copolymers after the PEGylation process in the same range as the molecular weights of the PEG chains being grafted. Furthermore, the absence of smaller polymer chains in the GPC chromatograms (data not shown) confirms the purification of the PEGylated copolymers from unreacted PEG chains.

The US-responsiveness of the copolymer after conjugation with PEG was checked by monitoring the LCST behavior before and after ultrasound exposure. The results show that our PUS-PEG presents a LCST below 37 ºC in water before the application of US (Figure 2). This behavior implies that at physiological temperature the polymer will be collapsed on the nanoparticle surface, effectively capping the pores and preventing the premature release of the drug. After US application, the LCST is shifted to values above 45 ºC. This change is due to the cleavage of the hydrophobic THPMA and its conversion to hydrophilic methacrylic acid, which induces a change in the overall hydrophilicity of the p(MEO_2MA-co-THPMA) block, displacing the LCST to a higher temperature.[24] The US-responsiveness of PUS-PEG was independent of its molecular weight (data not shown). This US-responsive behavior will provide the induced release capability in the final hybrid material.

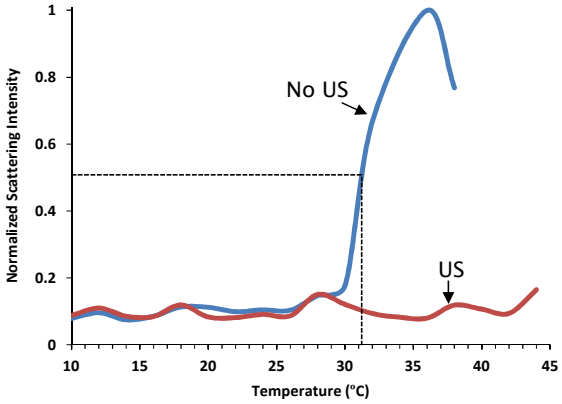

Figure 2. Lower critical solution temperature (LCST) of PUSL-PEG before (blue) and after 10 min (red) of ultrasound application (1.3MHz, 100 W, CW). A 1 mg/mL solution in water was used.

Once the US-responsiveness of PUS-PEG had been shown, it was then conjugated with APTES through its carboxylic acid (via DCC/NHS chemistry) and grafted to the surface of MSNs by condensation with the silanol groups of the silica particle,[24] as shown in Scheme 2.

Thus, we obtained different PEGylated hybrid materials, HYBRID-PEG, as a function of the molecular weight of the PUS-PEG grafted, as can be seen in Table 2. The organic matter percentage (determined by TGA) is similar (24-29 %) regardless of the molecular weight of the grafted polymer. However, significant differences can be found in the BET surface area, with decreasing values being obtained as the molecular weight of the polymers increased (Table 2, Figure S4).

View Article Online
DOI: 10.1039/C8TB00444G

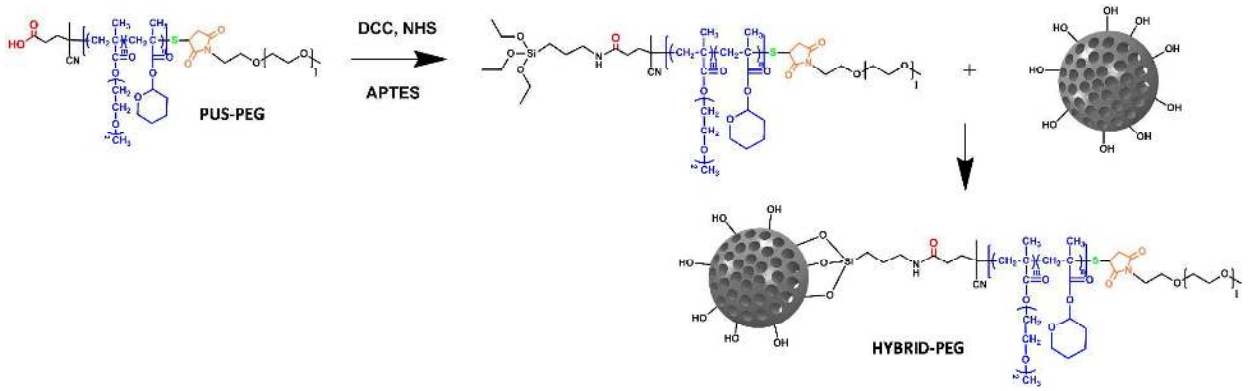

Scheme 2. Synthetic procedure employed to obtain the PEGylated Ultrasound-responsive material, Hybrid-PEG.

Table 2. Effect of molecular weight of the grafted copolymer on the organic matter %, BET surface area and % of dye released from HYBRID-PEG samples.

Samples	Organic matter % (TGA)	BET surface area (m^2/g)	Pore volume (cm^3/g)	% Fluorescein released after 20 h
HYBRID$_S$-PEG	24.9	634	0.55	80
HYBRID$_M$-PEG	24.0	585	0.39	45
HYBRID$_L$-PEG	28.8	188	0.13	23

The different HYBRID-PEG materials prepared were loaded with fluorescein. The percentage of dye released in PBS at 37 ºC was measured after 20 h to test if the PEGylated US-responsive polymers effectively block the pore entrances of the nanoparticles. Data collected in Table 2 indicates that the molecular weight of the RAFT polymer was found to be crucial on capping the pores to block premature cargo release. Thus, higher molecular weight led to less release of fluorescein. This result is in good agreement with previous work reported in the literature, showing that the molecular weight of polymers used as capping agents of MSNs drastically affects their efficiency.[32] Longer polymer chains form larger aggregates when they collapse on the surface of the silica particle, acting as a more effective capping agent (Table 2). This is also in agreement with BET surface areas mentioned above for those same materials. It is worth noting that the M_n needed to effectively cap the pores in this work is significantly higher than what we had seen in our preceding paper (around 28000 Da).[24]

This different behavior can be explained by the change in the polymer synthetic method. RAFT polymerization allows a much better control over the polymerization reaction compared to to FRP.[33] Thus, the molecular weight distribution of the copolymers obtained by RAFT polymerization was narrower than that obtained by FRP (PDI values around 2). Therefore, for the same M_n, the polymers obtained by FRP will present a significant percentage of polymer chains with a much larger size than the mean, which could have contributed to a better seal at the pore ends. According to these results, the hybrid material with the largest polymeric gate, HYBRID$_L$-PEG, was selected for all further experiments.

Once HYBRID$_L$-PEG had been selected, a more extensive characterization of the material further confirmed the successful grafting of PUS$_L$-PEG on the material surface. Figure 3 shows the TEM micrographs of MSNs and HYBRID$_L$-PEG, where the highly ordered mesoporous structure of the nanoparticles can be observed. Those same TEM micrographs of HYBRID$_L$-PEG (Figure 3) show a phosphotungstic acid-stained layer on the nanoparticle surface, which was not present on MSNs, corresponding to the polymeric gate, and confirming the successful grafting of the polymer to the nanoparticle surface. The FTIR spectrum of HYBRID$_L$-PEG (Figure 3) shows the typical bands of the polymer, between 1400 and 1800 cm^{-1}. The hydrodynamic diameter of HYBRID$_L$-PEG obtained by DLS indicates a peak size of 250 nm, with Z potential values of -45 mV (hydrodynamic diameter of MSNs was 220 nm with a Z potential value of -21 mV). These data confirm the correct grafting of a PEGylated polymeric gate capable of blocking premature cargo release from the mesopores of the material at physiological temperature.

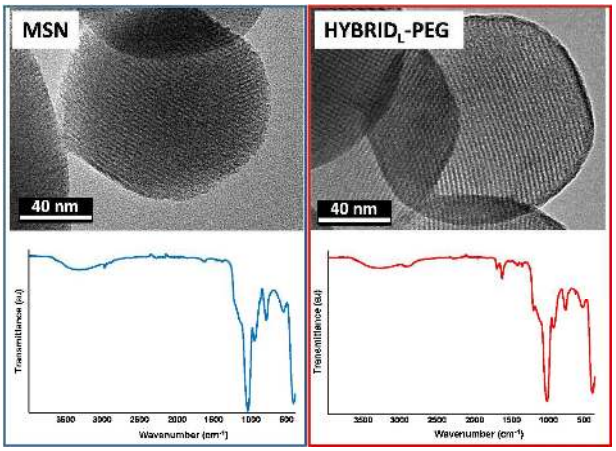

Figure 3. Characterization of MSNs (left) and HYBRID$_L$-PEG (right). TEM micrographs showing polymeric coating stained with PTA (top), FTIR spectra of the materials (bottom).

The stability of this new PEGylated hybrid material (HYBRID$_L$-PEG) was compared with our previously reported non-PEGylated hybrid material (HYBRID),[24] using FITC-labeled nanoparticles (Figure 4). The particles were dispersed in PBS (1

View Article Online
DOI: 10.1039/C8TB00444G

mg/mL of nanoparticles) and kept at 37 ºC for 1 h without stirring,to be then evaluated under visible and ultraviolet (UV) light. HYBRID nanoparticles can be clearly observed at the bottom of the cuvette (better assessed by the fluorescence of nanoparticles under UV light), while HYBRID$_L$-PEG nanoparticles remain much better dispersed. This enhancement in nanoparticle suspension stability was further confirmed by evaluating the hydrodynamic diameter of the PEGylated and the non-PEGylated system after different periods of time in suspension in 1 mM PBS (Figure S5). Non-PEGylated nanoparticles aggregated after 1 h in suspension, while the size of HYBRID$_L$-PEG remained unmodified for 6 h. These results indicate that the stability of the nanoparticle suspension was greatly improved in the PEGylated system, which was one of the main aims of our approach. Besides, PEGylation will extend nanoparticle circulation time after injection *in vivo*,[25,34] due to a slower withdrawal from the circulation by organs from the Mononuclear phagocyte system.

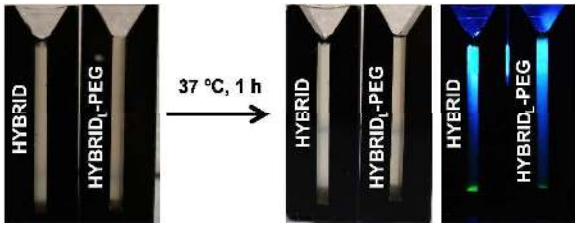

Figure 4. Suspension stability of HYBRID and HYBRID$_L$-PEG. Photographs taken under visible (left, center) or UV light (right).

Finally, the US-responsiveness of HYBRID$_L$-PEG was evaluated performing fluorescein release experiments. The material should be capable of retaining the cargo at 37 ºC, and releasing it in response to the application of US as an external stimulus. Figure 5 shows that fluorescein release was greatly enhanced when US is applied on a loaded HYBRID$_L$-PEG suspension.

These results indicate that the US-induced cargo release capability is retained in this PEGylated material, and its behavior is comparable to that obtained in our previous work.[24] This US-responsive behavior would enable the cargo to be released mostly in the tumor environment, improving the safety and efficacy profile of the system.

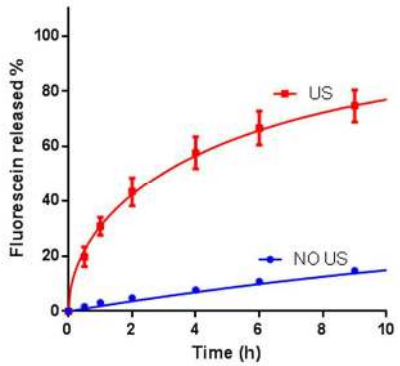

Figure 5. *In vitro* fluorescein release from HYBRID$_L$-PEG without or with US exposure (10 min, 1.3 MHz, 100 W, CW).

Targeted PEGylated Ultrasound-Responsive system

Heretofore, we have successfully obtained a PEGylated material that can trigger the release of its cargo when exposed to US. However, no active targeting strategy had been implemented to enhance the specificity of this material. To address the need for active targeting molecules, a different hybrid material was obtained by a similar process, but employing a PEG chain with biotin at one end (as targeting agent) and a maleimide at the other end (as coupling moiety), MAL-PEG-BIOTIN (Scheme 3). Consequently, the biotin moiety will be present on the end of the PEG chain attached to the polymeric gate on the nanoparticle surface. Biotin, also known as vitamin B7, can be employed as an active targeting agent due to the overexpression of biotin receptors by a variety of cancer cells.[35] While the TGA data did not allow us to estimate the amount of biotin in HYBRID$_L$-PEG-BIOTIN (Figure S4), such quantification was possible through the HABA/Avidin test. The value obtained (2.13 nmol biotin/mg of nanoparticles) was in close agreement with the value expected from the organic matter % (determined by TGA) and the M_n of the attached polymer.

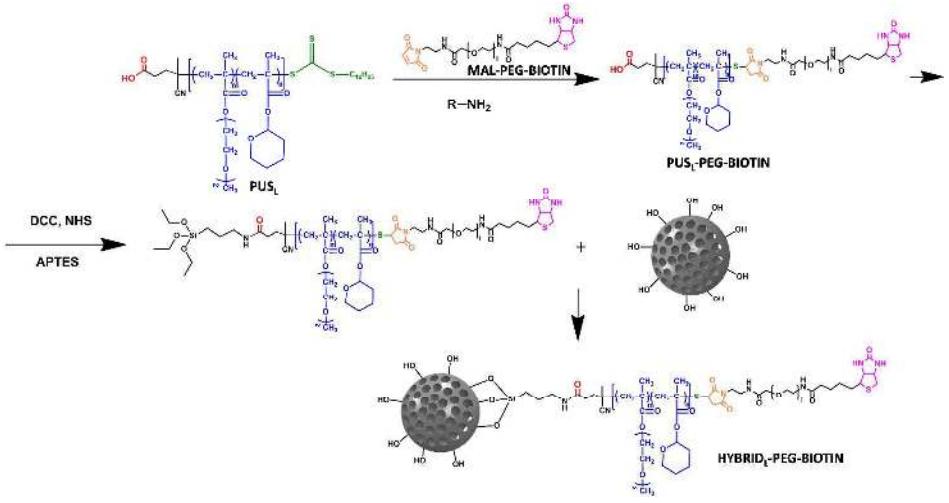

Scheme 3. Synthetic procedure employed to obtain the PEGylated, biotin-targeted ultrasound-responsive material, HYBRID$_L$-PEG-BIOTIN.

View Article Online
DOI: 10.1039/C8TB00444G

An *in vitro* cellular uptake experiment was performed to test the efficacy of the biotin molecules exposed by our nanoparticles as active targeting agents. Incubation of non-targeted and targeted PEGylated nanoparticles (HYBRID$_L$-PEG and HYBRID$_L$-PEG-BIOTIN) with HeLa cells, which have been reported to overexpress biotin receptors,[36] shows a significantly increased cellular uptake of biotin-modified nanoparticles, as can be seen from fluorescence microscopy and flow cytometry data (Figure 6).

These results confirm the possibility to attach a targeting moiety to the external surface of our US-responsive nanocarrier, allowing a selective delivery to specific types of cancer cells. However, the chemical strategies employed to obtain our final system, limit the amount of targeting agents that can be conjugated to the PEG chain before it is coupled with the polymeric gate and then grafted to the particles. Any molecule possessing free amines, carboxylic acids, thiols or maleimides can interfere with the subsequent reactions, giving rise to undesired side-products, and limiting the presented approach.

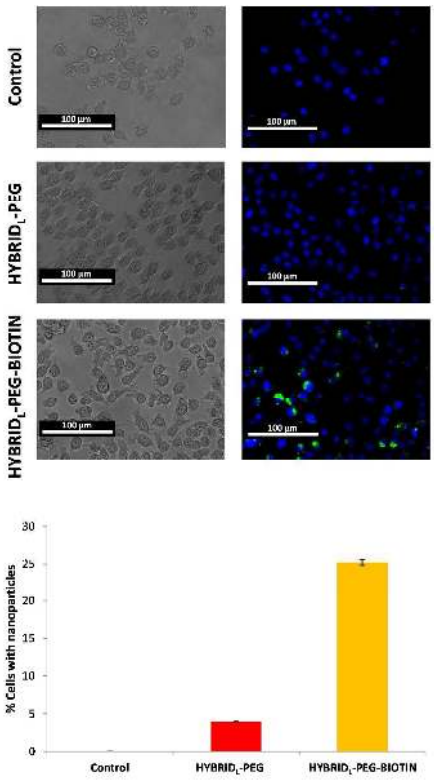

Figure 6. Uptake experiments in HeLa cells comparing HYBRID$_L$-PEG and HYBRID$_L$-PEG-BIOTIN by fluorescence microscopy (top, showing cell nuclei in blue and nanoparticles in green) and flow cytometry (bottom).

A modular device was designed to provide more versatility to our US-responsive system. Our approach consisted on conjugating a strained alkyne (the dibenzocyclooctyne or DBCO moiety) to a PEG molecule, which also presents a maleimide group in the other end, MAL-PEG-DBCO. This would allow carrying out the grafting process as already described (Scheme S1), and then coupling the desired targeting agent to the already prepared hybrid system, HYBRID$_L$-PEG-DBCO, by using a copper-free alkyne-azidecyclo addition. The DBCO moiety will react with azide-functionalized molecules to yield a stable triazole linkage.

Before grafting any targeting molecules, a coupling reaction with an azide-dye (TAMRA-N_3) was performed to ensure the presence and availability of the DBCO moiety in the material (Supporting Information). That way, sample color and/or fluorescence could be used to test if the click reaction has taken place. After reaction of HYBRID-PEG-DBCO with TAMRA-N_3, sample fluorescence indicates a successful reaction with the dye (Figure S6). Same results were obtained with the intermediate products (MAL-PEG-DBCO, PUS$_L$-PEG-DBCO). This demonstrates the correct coupling of DBCO and that it is available to react through click chemistry. On the other hand, no reaction with the dye took place in the materials not carrying DBCO. All of these results indicate that it is possible to graft an azide-modified molecule to our HYBRID$_L$-PEG-DBCO. These data open the gate for endless easy modifications of the material, fine-tuning the targeting capacity of the system towards specific cell lines, once the US-responsive material has already been prepared.

The versatility of this methodology has been tested by attaching a targeting agent to HYBRID$_L$-PEG-DBCO and evaluating its cellular uptake. A peptide containing the RGD (Arg-Gly-Asp) sequence was used as the active targeting agent to be anchored to HYBRID$_L$-PEG-DBCO. This sequence is selectively recognized by αvβ3 integrin receptor, and has been extensively studied as an active targeting agent for anticancer therapies.[37] Several functional groups present in this sequence (like amines and carboxylic acids) would impede the inclusion of this peptide in the PEGylated polymeric gate, due to incompatibility issues with the polymer grafting methodology above described. For this reason, the RGD sequence was attached to HYBRID$_L$-PEG-DBCO by copper-free azide-alkyne cycloaddition using an azide-functionalized peptide, RGD-N_3 (Scheme S2) to obtain HYBRID$_L$-PEG-RGD (Figure 7).

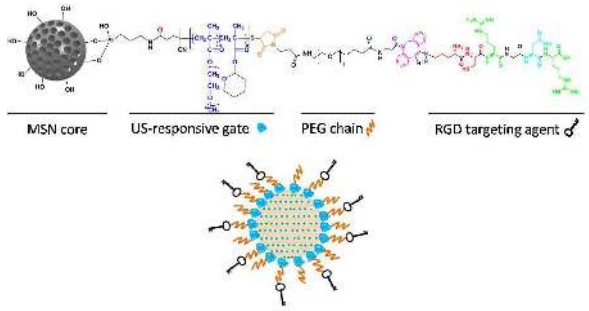

Figure 7. Structure of the obtained PEGylated RGD-targeted US-responsive hybrid mesoporous silica nanoparticles, HYBRID$_L$-PEG-RGD.

Cellular uptake studies were carried out with HeLa cells, which also overexpress integrins capable of interacting with the RGD

View Article Online
DOI: 10.1039/C8TB00444G

sequence.[38] Figure 8 shows a significantly increased uptake in RGD-containing nanoparticles (HYBRID$_L$-PEG-RGD). This result highlights the successful development of our modular strategy to obtain an actively-targeted material. Further, a competition assay with the addition of free RGD in the medium shows a decrease in the internalization of HYBRID$_L$-PEG-RGD, indicating a receptor-mediated uptake mechanism.

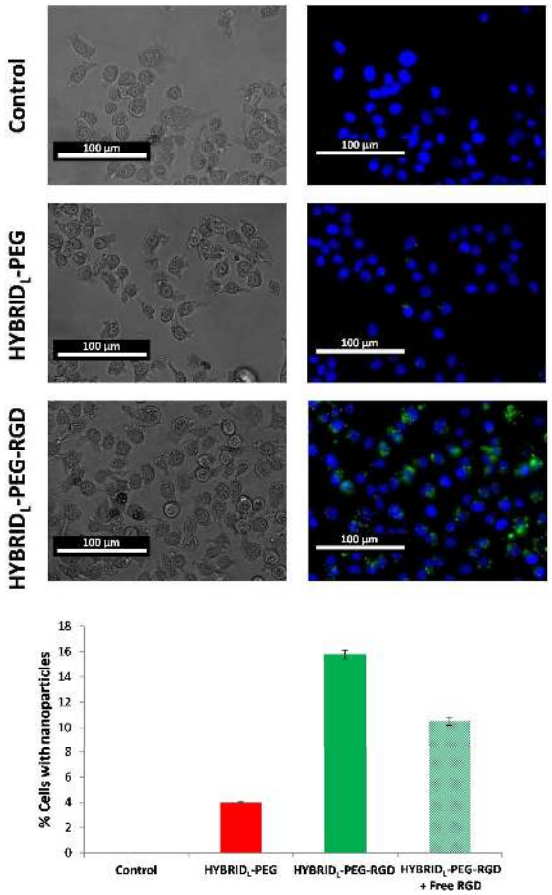

Figure 8. Uptake experiments in HeLa cells comparing HYBRID$_L$-PEG and HYBRID$_L$-PEG-RGD by fluorescence microscopy (top, showing cell nuclei in blue and nanoparticles in green) and flow cytometry (bottom).

Finally, and since the material presented in this work is aimed for anticancer therapy, these actively-targeted nanoparticles must be able to kill cancer cells upon US exposure when loaded with a cytotoxic drug. According to the cellular uptake results, the targeted system (HYBRID$_L$-PEG-RGD) was selected for our cytotoxicity experiment with drug-loaded nanoparticles. Doxorubicin-loaded HYBRID$_L$-PEG-RGD nanoparticles were incubated with HeLa cells overnight. The cells were then washed with PBS to remove non-internalized nanoparticles, in order to try to only evaluate the effect on cell viability of nanoparticles that will release the drug within the cancer cell. Some of the cells were then exposed to ultrasound using a physiotherapy device, and cell viability was evaluated by Alamar Blue test over the next three days (Figure 9). Ultrasound itself was shown not to have any significant effect on cell viability. Ultrasound-exposed nanoparticles showed significantly higher cytotoxicity on HeLa cells than the nanoparticles not exposed to the stimulus, denoting the greater doxorubicin release upon US application. This further indicates that we have obtained a PEGylated, modularly-targeted, ultrasound responsive drug carrier with great potential in the field of cancer nanomedicine. Nanoparticle uptake by the target cancer cells will be enhanced by the addition of an active targeting molecule, and the external application of ultrasound in the tumor area will induce the release of the cytotoxic drug loaded in the nanoparticle, killing the cancer cells while decreasing the undesired side effects of chemotherapy.

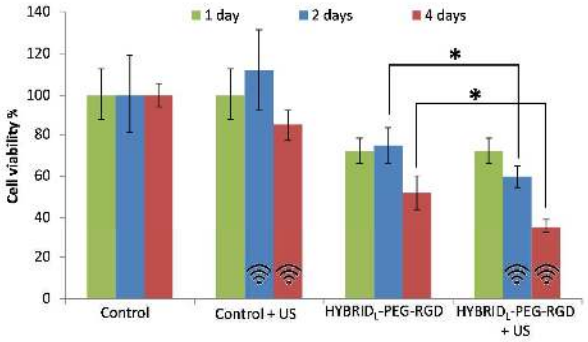

Figure 9. Cytotoxicity assay measured by Alamar Blue test in HeLa cells at different time points (1, 2 and 4 days) after incubation with doxorubicin-loaded HYBRIDL-PEG-RGD. Samples without US exposure and with US exposure (1 MHz, 3 W/cm2, 5 min, CW) were evaluated (US was applied after measuring the 1 day time point). *p < 0.05 (Student's t-test).

Conclusions

A PEGylated and targeted modular ultrasound-responsive nanocarrier based on Mesoporous Silica Nanoparticles has been successfully obtained. To prepare this material, we had to develop a new set of chemical strategies, since previously reported methods were not suitable to afford this versatile stimulus-responsive nanocarrier.

First, a non-targeted PEGylated material possessing ultrasound-promoted cargo release was obtained and characterized. That PEGylated material showed increased stability in aqueous suspension when compared to its non-PEGylated control, which is of great interest for its biomedical application.

By further modifying the material, a modular nanocarrier was obtained, in which any targeting agent could be easily attached to the final system through click chemistry. By taking advantage of that modularity of the material, RGD-decorated nanoparticles were obtained and demonstrated to induce enhanced cellular uptake. Drug-loaded RGD-targeted PEGylated nanoparticles were shown to produce significantly increased cancer cell killing when exposed to ultrasound.

Conflicts of interest

There are no conflicts to declare.

View Article Online
DOI: 10.1039/C8TB00444G

Acknowledgements

The authors thank the funding from the European Research Council through the Advanced Grant VERDI (ERC-2015 AdG proposal no. 694160). Financial support from Ministerio de Economía y Competitividad, (MEC), Spain (Project MAT2015-64831-R) is gratefully acknowledged. JL Paris gratefully acknowledges MEC, Spain, for his PhD grant (BES-2013-064182).

References

1 A. Wicki, D. Witzigmann, V. Balasubramanian and J. Huwyler, *J. Control. Release*, 2015, **200**, 138–157.
2 H. Ragelle, F. Danhier, V. Préat, R. Langer and D. G. Anderson, *Expert Opin. Drug Deliv.*, 2017, **14**, 851–864.
3 J. Fang, H. Nakamura and H. Maeda, *Adv. Drug Deliv. Rev.*, 2011, **63**, 136–151.
4 N. Bertrand, J. Wu, X. Xu, N. Kamaly and O. C. Farokhzad, *Adv. Drug Deliv. Rev.*, 2014, **66**, 2–25.
5 S. Mura, J. Nicolas and P. Couvreur, *Nat. Mater.*, 2013, **12**, 991–1003.
6 Y. Chen, K. Ai, J. Liu, G. Sun, Q. Yin and L. Lu, *Biomaterials*, 2015, **60**, 111–120.
7 N. Song, W. Liu, Q. Tu, R. Liu, Y. Zhang and J. Wang, *Colloids Surf. B. Biointerfaces*, 2011, **87**, 454–63.
8 J. Lai, X. Mu, Y. Xu, X. Wu, C. Wu, C. Li, J. Chen and Y. Zhao, *Chem. Commun.*, 2010, **46**, 7370–7372.
9 E. Guisasola, A. Baeza, M. Talelli, D. Arcos, M. Moros, J. M. de la Fuente and M. Vallet-Regí, *Langmuir*, 2015, **31**, 12777–12782.
10 S. R. Sirsi and M. A. Borden, *Adv. Drug Deliv. Rev.*, 2014, **72**, 3–14.
11 P. Huang, X. Qian, Y. Chen, L. Yu, H. Lin, L. Wang, Y. Zhu and J. Shi, *J. Am. Chem. Soc.*, 2017, **139**, 1275–1284.
12 Y. Xu, Y. Zhu and S. Kaskel, *RSC Adv.*, 2015, **5**, 99875–99883.
13 X. Yao, X. Niu, K. Ma, P. Huang, J. Grothe, S. Kaskel and Y. Zhu, *Small*, 2017, **13**, 1602225.
14 X. Yao, Z. Tian, J. Liu, Y. Zhu and N. Hanagata, *Langmuir*, 2017, **33**, 591–599.
15 J. Chen, H. Luo, Y. Liu, W. Zhang, H. Li, T. Luo, K. Zhang, Y. Zhao and J. Liu, *ACS Nano*, 2017, **11**, 12849–12862.
16 K. Zhang, H. Xu, H. Chen, X. Jia, S. Zheng, X. Cai, R. Wang, J. Mou, Y. Zheng and J. Shi, *Theranostics*, 2015, **5**, 1291–1302.
17 K. Zhang, H. Chen, F. Li, Q. Wang, S. Zheng, H. Xu, M. Ma, X. Jia, Y. Chen, J. Mou, X. Wang and J. Shi, *Biomaterials*, 2014, **35**, 5875–5885.
18 K. Zhang, H. Xu, X. Jia, Y. Chen, M. Ma, L. Sun and H. Chen, *ACS Nano*, 2016, **10**, 10816–10828.
19 M. Vallet-Regí, A. Rámila, R. P. del Real and J. Pérez-Pariente, *Chem. Mater.*, 2001, **13**, 308–311.
20 C. Argyo, V. Weiss, C. Bräuchle and T. Bein, *Chem. Mater.*, 2014, **26**, 435–451.
21 X. Yu and Y. Zhu, *Sci. Technol. Adv. Mater.*, 2016, **17**, 229–238.
22 K. Zhang, H. Chen, Y. Zheng, Y. Chen, M. Ma, X. Wang, L. Wang, D. Zeng and J. Shi, *J. Mater. Chem.*, 2012, **22**, 12553.
23 M. Ma, S. Zheng, H. Chen, M. Yao, K. Zhang, X. Jia, J. Mou, H. Xu, R. Wu and J. Shi, *J. Mater. Chem. B*, 2014, **2**, 5828–5836.
24 J. L. Paris, M. V. Cabañas, M. Manzano and M. Vallet-Regí, *ACS Nano*, 2015, **9**, 11023–11033.
25 V. Cauda, C. Argyo and T. Bein, *J. Mater. Chem.*, 2010, **20**, 8693–8699.
26 A. Baeza, M. Manzano, M. Colilla and M. Vallet-Regí, *Biomater. Sci.*, 2016, **4**, 803–813.
27 J.-T. Lee, M. C. George, J. S. Moore and P. V Braun, *J. Am. Chem. Soc.*, 2009, **131**, 11294–11295.
28 C. Boyer, A. Granville, T. P. Davis and V. Bulmus, *J. Polym. Sci. Part A Polym. Chem.*, 2009, **47**, 3773–3794.
29 X. P. Qiu and F. M. Winnik, *Macromol. Rapid Commun.*, 2006, **27**, 1648–1653.
30 J. Xuan, O. Boissière, Y. Zhao, B. Yan, L. Tremblay, S. Lacelle, H. Xia and Y. Zhao, *Langmuir*, 2012, **28**, 16463–16468.
31 J. Chen, M. Liu, C. Chen, H. Gong and C. Gao, *ACS Appl. Mater. Interfaces*, 2011, **3**, 3215–3223.
32 A. Popat, J. Liu, G. Q. Lu and S. Z. Qiao, *J. Mater. Chem.*, 2012, **22**, 11173–11178.
33 R. Liu, M. Fraylich and B. R. Saunders, *Colloid Polym. Sci.*, 2009, **287**, 627–643.
34 Q. He, J. Zhang, J. Shi, Z. Zhu, L. Zhang, W. Bu, L. Guo and Y. Chen, *Biomaterials*, 2010, **31**, 1085–1092.
35 W. X. Ren, J. Han, S. Uhm, Y. J. Jang, C. Kang, J.-H. Kim and J. S. Kim, *Chem. Commun.*, 2015, **51**, 10403–10418.
36 W. Yang, Y. Cheng, T. Xu, X. Wang and L. P. Wen, *Eur. J. Med. Chem.*, 2009, **44**, 862–868.
37 A. Accardo, D. Tesauro and G. Morelli, *Polym. J.*, 2013, **45**, 481–493.
38 M. Oba, K. Aoyagi, K. Miyata, Y. Matsumoto, K. Itaka, N. Nishiyama, Y. Yamasaki, H. Koyama and K. Kataoka, *Mol. Pharm.*, 2008, **5**, 1080–1092.

View Article Online
DOI: 10.1039/C8TB00444G

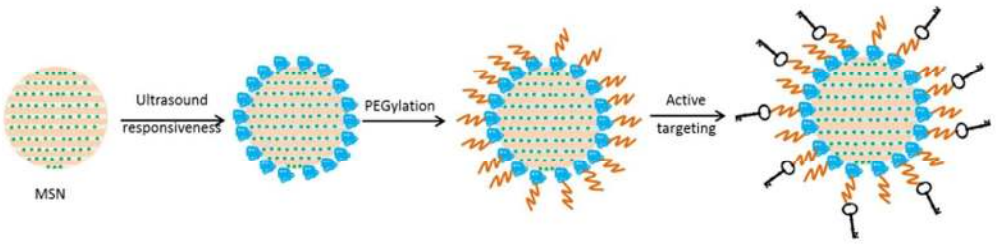

A modularly-targeted, PEGylated and ultrasound-responsive hybrid nanomaterial is here prepared. Starting from naked mesoporous silica nanoparticles, we describe the synthetic method to obtain this hybrid material, also carrying out its characterization and *in vitro* evaluation.